Human Molecular Genetics, 2012, Vol. 21, No. 4 **916–925**
doi:10.1093/hmg/ddr528
Advance Access published on November 11, 2011

Abnormal nuclear envelopes in the striatum and motor deficits in DYT11 myoclonus-dystonia mouse models

Fumiaki Yokoi[1], Mai T. Dang[2], Tong Zhou[3] and Yuqing Li[1,*]

[1]Department of Neurology, College of Medicine, University of Florida, Gainesville, FL 32610-0236, USA, [2]Department of Neurology, Hospital of University of Pennsylvania, Philadelphia, PA 19104, USA and [3]Clinical Immunology and Rheumatology, Department of Medicine, School of Medicine, University of Alabama at Birmingham, Birmingham, AL 35294-2182, USA

Received October 13, 2011; Revised October 13, 2011; Accepted November 7, 2011

DYT11 myoclonus-dystonia (M-D) is a movement disorder characterized by myoclonic jerks with dystonic symptoms and caused by mutations in paternally expressed *SGCE*, which codes for ε-sarcoglycan. Paternally inherited *Sgce* heterozygous knock-out (KO) mice exhibit motor deficits and spontaneous myoclonus. Abnormal nuclear envelopes have been reported in cellular and mouse models of early-onset DYT1 generalized torsion dystonia; however, the relationship between the abnormal nuclear envelopes and motor symptoms are not clear. Furthermore, it is not known whether abnormal nuclear envelope exists in non-DYT1 dystonia. In the present study, abnormal nuclear envelopes in the striatal medium spiny neurons (MSNs) were found in *Sgce* KO mice. To analyze whether the loss of ε-sarcoglycan in the striatum alone causes abnormal nuclear envelopes, motor deficits or myoclonus, we produced paternally inherited striatum-specific *Sgce* conditional KO (*Sgce* sKO) mice and analyzed their phenotypes. *Sgce* sKO mice exhibited motor deficits in both beam-walking and accelerated rotarod tests, while they did not exhibit abnormal nuclear envelopes, alteration in locomotion, or myoclonus. The results suggest that the loss of ε-sarcoglycan in the striatum contributes to motor deficits, while it alone does not produce abnormal nuclear envelopes or myoclonus. Development of therapies targeting the striatum to compensate for the loss of ε-sarcoglycan function may rescue the motor deficits in DYT11 M-D patients.

INTRODUCTION

Dystonia is a movement disorder characterized by involuntary, repetitive, sustained muscle contractions or postures (1). Dystonia is classified into two groups, primary and secondary (2). Primary dystonia develops spontaneously in absence of any apparent cause or associated disease. Secondary dystonia is mainly caused by other disease states or brain injury. Genetic dystonia belongs to the primary dystonia and is classified into at least 20 types, although less than half of them have known gene mutations (2–4). Myoclonus is a sudden brief jerk caused by involuntary muscle activity (5). Myoclonus-dystonia (M-D) is a movement disorder characterized by myoclonic jerks with dystonic symptoms (6). M-D itself is genetically heterogeneous and DYT11 M-D is a major type of genetic M-D (7,8).

DYT11 M-D is linked to mutations in *SGCE* which codes for ε-sarcoglycan (9). Sarcoglycans are transmembrane glycoproteins with six different isoforms—α, β, γ, δ, ε and ζ (10). α-, β-, γ- and δ-sarcoglycans form a sarcoglycan complex. Loss of a member of this complex causes significant reduction in all members of the complex in skeletal muscles via a mechanism known as sarcoglycanopathy hypothesis (11). Mutations in the genes coding for α-, β-, γ- and δ-sarcoglycans cause limb-girdle muscular dystrophies (12). ζ-Sarcoglycan is also a member of the sarcoglycan complex in skeletal muscle and is reduced in γ-sarcoglycan-deficient mice (13).

ε-Sarcoglycan has been identified in the mouse as an α-sarcoglycan homolog (14). The cDNA clones coding for ε-sarcoglycan have been reported in the mouse (14–17), human (18,19) and rat (20). The protein sequence homology

*To whom correspondence should be addressed. Tel: +1 3522736546; Fax: +1 3522735989; Email: yuqingli@ufl.edu

analysis and 3D structure modeling predict that α- and ε-sarcoglycans have cadherin-like domains at their *N*-terminal extracellular regions, suggesting they may be necessary for intercellular adhesion, including synaptic formation and maintenance (21). ε-Sarcoglycan is widely expressed in the body, such as in the brain, heart, lung and smooth muscles (14,18). Mouse ε-sarcoglycan has alternative splicing variants and brain-specific isoforms have PSD95/Dlg/ZO-1 (PDZ)-binding motifs (17). PDZ-containing proteins are typically involved in the assembly of supramolecular complexes that perform localized signaling functions at particular subcellular locations (22). The ε-sarcoglycan variants may be incorporated into supramolecular complexes in the synapse by the PDZ-binding motif. A loss of PDZ-binding motifs may interfere with the binding of ε-sarcoglycan to its interacting proteins. Mouse ε-sarcoglycan is enriched in pre- and post-synaptic membrane fractions from the brains, suggesting it may also function in synaptic transmission (16). Immunoprecipitation analysis suggested that four types of sarcoglycan complexes (α–β–γ–δ, α–β–ζ–δ, ε–β–γ–δ and ε–β–ζ–δ) associated with dystroglycan can be constructed at the plasma membrane by using expression vectors in Chinese hamster ovary (CHO) cells. This further suggests that ε-sarcoglycan is a functional homolog of α-sarcoglycan, while ζ-sarcoglycan is a functional homolog of γ-sarcoglycan (23).

The gene for ε-sarcoglycan is maternally imprinted and paternally expressed in both humans and mice (17,24–27). However, *de novo SGCE* mutations were also reported in DYT11 M-D patients (28). Majority of the DYT11 patients have a paternal *SGCE* mutation. We previously reported the generation of *Sgce* knock-out (KO) mice lacking exon 4 and demonstrated that paternally inherited *Sgce* heterozygous KO mice do not express maternally inherited wild-type (WT) *Sgce* in their brains (17). Therefore, we used these heterozygotes as *Sgce* KO mice in our studies. *Sgce* KO mice exhibited spontaneous myoclonus, motor deficits in the beam-walking test, alterations of the emotional response and monoamine metabolism in the striatum, suggesting functional alterations of the striatum may contribute to the pathogenesis of DYT11 M-D (29).

It has been believed that dystonia has a functional rather than neurodegenerative etiology. Recent studies suggested that there are functional microstructural brain alterations without overt neurodegeneration in another type of dystonia, specifically in DYT1 generalized torsion dystonia patients (30) and its mouse model (31). Abnormal nuclear envelopes were reported in both *in vitro* and *in vivo* models of DYT1 dystonia. Additionally, over-expression of mutant torsinA leads to abnormal nuclear envelopes in transfected cells (32–34). TorsinA binds to nesprins and participates in linkage between the nuclear envelope and the cytoskeleton (35). Abnormal nuclear envelopes in neurons were also reported in DYT1 dystonia mouse models (36–38). A recent study suggested that lamina-associated polypeptide 1 and torsinB function with torsinA to maintain normal nuclear membrane morphology (39). However, abnormal envelopes were detected only in newborn *Tor1a* $^{\Delta gag/\Delta gag}$ (*Dyt1* ΔGAG homozygous knock-in) mice or KO mice and were not detected in *Dyt1* ΔGAG heterozygous KI mice, while only heterozygous mutations have been reported in human mutation carriers (36). Moreover, both transgenic mice over-expressing human WT torsinA and *Dyt1* ΔGAG mutant form of torsinA (torsinA$^{\Delta E}$) exhibit motor deficits and abnormal nuclear envelopes (37). Therefore, the relationships between the mutation, abnormal nuclear envelopes and motor symptoms are not clear in DYT1 dystonia. Furthermore, it was not known whether abnormal nuclear envelope exists in non-DYT1 dystonia. Nuclear envelope abnormality has not been examined in DYT11 M-D because of the difficulty of obtaining patient brains.

The striatum is a key player in motor function. Many movement disorders related to dystonia are caused by dysfunction of this region. Parkinson's disease, for example, is caused by neurodegeneration of dopaminergic neurons which innervate the striatal neurons. Dystonic symptoms are often observed at the early stage of Parkinson's disease (40). Additionally, Huntington's disease is caused by neurodegeneration of the striatal neurons and dystonic symptoms are also observed in this disease (41). Pathological alterations precede the overt onset of clinical symptoms in Parkinson's (42) and Huntington's disease (43). In these neurodegenerative disorders, contribution of the striatum to the motor symptoms is clear. However, dystonia is not caused by overt neurodegeneration, so the involvement of the striatum in dystonia's pathology is not clear and more detailed analysis for circuitry abnormality and/or cellular dysfunction is needed. DYT5 dopa-responsive dystonia is caused by failure of producing enough dopamine which works to innervate striatal neurons (44). Functional alterations of the striatum were also reported in the DYT1 dystonia patients (45) and mouse models (38,46–48). Reduced striatal D2 binding were reported in *SGCE* mutation carriers (49).

Here we analyzed the levels of other sarcoglycans to determine whether the loss of ε-sarcoglycan affects the levels of other sarcoglycan members and the nuclear envelopes in *Sgce* KO mouse striata. To investigate whether the loss of ε-sarcoglycan in the striatum alone causes the motor deficits, myoclonus or abnormal nuclear envelope, we produced paternally inherited striatum-specific *Sgce* conditional knock-out (*Sgce* sKO) mice and analyzed these phenotypes.

RESULTS

Loss of ε-sarcoglycan does not affect α-sarcoglycan, δ-sarcoglycan or ζ-sarcoglycan levels in the striatum

To elucidate whether the loss of ε-sarcoglycan affects the levels of other sarcoglycan members in the mouse striatum, we analyzed the levels of α-, δ- and ζ-sarcoglycan by western blot. There was no significant difference in the levels of α- (Fig. 1A; $P = 0.46$), δ- (Fig. 1B; $P = 0.25$) or ζ-sarcoglycan (Fig. 1C; $P = 0.48$), suggesting the loss of ε-sarcoglycan did not affect the expression levels of α-, δ- or ζ-sarcoglycan in the mouse striatum.

Abnormal nuclear envelopes of the striatal MSNs in adult *Sgce* KO mice

Sgce KO mice and their WT littermates were produced as described previously (17) and nuclear envelopes in the striatal neurons were examined using a transmission electron

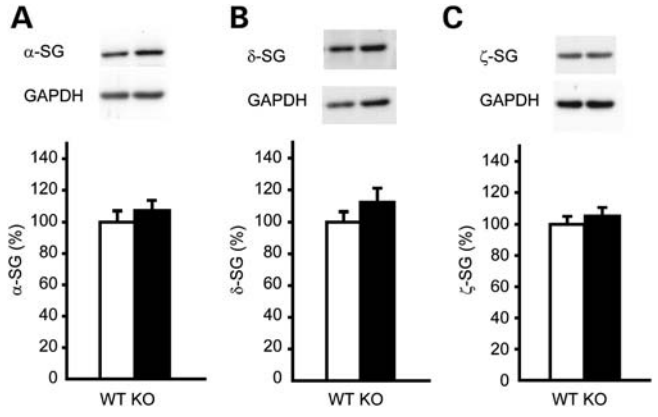

Figure 1. The amounts of α-sarcoglycan, δ-sarcoglycan and ζ-sarcoglycan in the striatal protein extracts from *Sgce* KO mice and WT littermates. The representative bands are shown on the top of each graph and the quantified α-sarcoglycan (α-SG), δ-sarcoglycan (δ-SG) and ζ-sarcoglycan (ζ-SG) are shown under the images (**A**–**C**, respectively). The vertical bars represent means ± standard errors (SE).

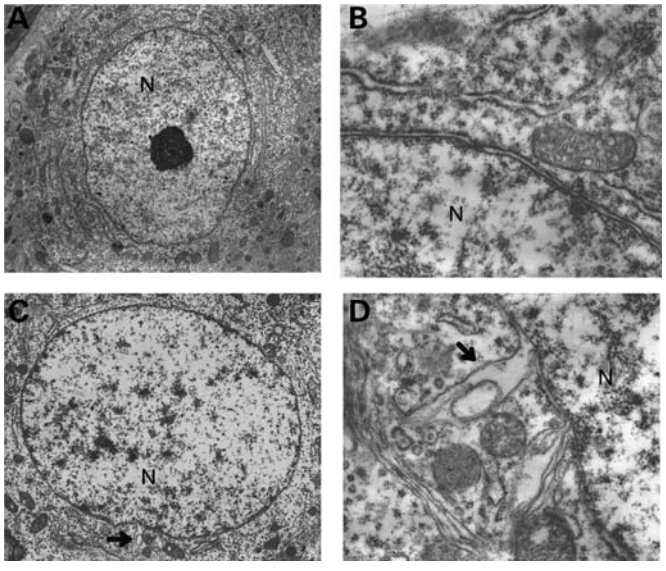

Figure 2. Nuclear envelope structures in WT littermates (**A** and **B**) and *Sgce* KO (**C** and **D**) mice. Although abnormal nuclear envelope in the striatum was not detected in WT littermates (A and B), it was found in *Sgce* KO mice (C and D). Arrows indicate abnormal nuclear envelopes in (C) and (D). Nucleus is shown as *N* in (A–D). Magnifications: (A) and (C) are 5 k ×; (B) and (D) are 25k ×. Representative electron microscope images are shown.

microscope. Although no abnormal nuclear envelopes were detected in the 111 sections examined from six WT mice (Fig. 2A and B), 21 abnormal nuclear envelopes were detected in the 118 medium spiny neuron (MSN) sections examined from six *Sgce* KO mice (Fig. 2C). Numbers of MSN sections with abnormal nuclear envelopes in *Sgce* KO mice were significantly higher than those in WT mice ($\chi^2 = 21.74$, $P = 0.000003$). Detailed analysis (Fig. 2D) revealed that nuclear envelope blebbing and other nuclear envelope abnormalities were similar to those reported in DYT1 dystonia models. Abnormal envelopes were detected in the sections of *Sgce* KO mice at 2–5.5 months old, well in advance of the onset of motor deficits in the beam-walking test at ∼6.5 months old (50). All mice examined were adults and unlike DYT1 mouse models, abnormal nuclear envelopes should not be relating to the neuronal cell death during the development. Our results suggest that the abnormal envelope may be a pathological biomarker of the defected brain region that appears in advance of the onset of motor symptoms in DYT11 dystonia. On the other hand, obvious structural alterations in the cytoplasm were not found in the sections from *Sgce* KO mice or their WT littermates.

Generation of *Sgce* sKO mice

To analyze whether the loss of ε-sarcoglycan in the striatum alone causes motor deficits, myoclonus or abnormal nuclear envelope, we used *cre-loxP* technology (51) applied to mouse gene recombination (52) to selectively inactivate *Sgce* in the striatum. This is made possible by using an *Rgs9-cre* line that has restricted expression in the striatum (53). *Sgce* sKO mice and their littermates were produced by crossing *Sgce loxP* male mice (17) with *Rgs9-cre* female mice (Fig. 3A). Genotyping was performed by multiplex polymerase chain reaction (PCR) with the tail DNA (Fig. 3B). Striatum-specific deletion of *Sgce* exon 4 in *Sgce* sKO mice was confirmed by PCR using DNA isolated from several brain regions. The deletion of *Sgce* exon 4 was detected only in the striatum as predicted (Fig. 3C). Coronal sections of control (Fig. 4A) and *Sgce* sKO (Fig. 4B) mouse brains were stained by immunohistochemistry using a monoclonal antibody against mouse ε-sarcoglycan, which we developed recently (50), and the striatum-specific reduction in ε-sarcoglycan was confirmed. Enlarged images suggested that the neurons in both cerebral cortices of control (Fig. 4C) and *Sgce* sKO mice (Fig. 4D) were similarly stained. On the other hand, while the striatal MSNs were stained in control mice (Fig. 4E), the corresponding neurons were not well stained in the striatum of *Sgce* sKO mice (Fig. 4F), suggesting striatum-specific loss of ε-sarcoglycan in *Sgce* sKO mice as predicted. *Sgce* sKO mice were born according to the Mendelian ratio and developed to adults.

Normal nuclear envelopes of the striatum in *Sgce* sKO mice

Since *Sgce* KO mice showed abnormal nuclear envelopes in MSNs, we further examined nuclear envelopes of MSNs in *Sgce* sKO mice using a transmission electron microscope to determine whether abnormal nuclear envelopes were caused by a cell-autonomous phenomenon in the absence of ε-sarcoglycan in the MSNs alone. There were no blebbing of MSNs in the examined 141 sections of control littermate mice as predicted ($n = 3$; Fig. 5A and B). We could not find the nuclear envelope abnormalities either in the examined 201 MSN sections from *Sgce* sKO mice ($n = 3$; Fig. 5C and D). The results suggest that the loss of ε-sarcoglycan in MSNs alone does produce the nuclear envelope abnormalities.

No overt abnormal postures in *Sgce* sKO mice

Posture abnormality was examined as previously described (46,54). When suspended from the tail, both *Sgce* sKO and

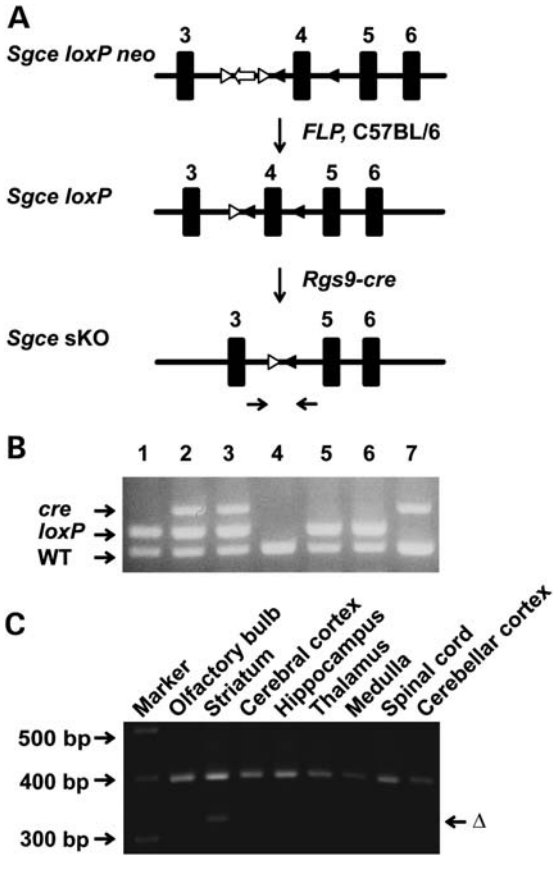

Figure 3. Generation of *Sgce* sKO mice. (**A**) Strategies to generate *Sgce* sKO mice. *Sgce loxP neo* mice were prepared as described previously (17). *Neo* cassette was removed by crossing with *FLP* mice. *FLP* was removed by backcrossing to C57BL/6 mice to produce *Sgce loxP* mice. *Sgce loxP* male mice were crossed with *Rgs9-cre* female mice to produce *Sgce* sKO mice. The primer sites to amplify the exon 4-deleted locus (Δ) were shown by the arrow pair under the map. (**B**) A representative image of multiplex PCR-based genotyping. Top band is PCR product from *cre*. Middle band is for *Sgce loxP* locus and the bottom band is the *Sgce* WT locus. Lanes 1, 5, 6: *Sgce loxP* heterozygous mice; lanes 2, 3: *Sgce* sKO mice; lane 4: WT mouse; lane 7: *Rgs9-cre* mouse. (**C**) Striatum-specific deletion of *Sgce* exon 4 in *Sgce* sKO mice was confirmed by PCR using DNA isolated from each brain region. Top bands were PCR products of dopamine transporter gene as an internal control. The deletion of *Sgce* exon 4 (Δ) was detected only in the striatum as predicted.

control littermate mice have normal splaying of hindpaws. *Sgce* sKO mice had no observable hindpaw extension or truncal arching compared with their control littermates. All mice exhibited strong righting reflexes when tipped on their side. The results suggest that *Sgce* sKO mice had no overt abnormal postures, similar to the *Sgce* KO mice (29).

No significant alteration in locomotion of *Sgce* sKO mice

Spontaneous activities in *Sgce* sKO mice were examined in an open-field apparatus and compared with those in control littermates (Table 1). *Sgce* sKO mice did not exhibit significant differences in comparison to control littermates in horizontal locomotion (horizontal activity, total distance, horizontal movement number or movement time), clockwise or anticlockwise revolutions, or stereotypic behaviors (stereotypic activity, movement number or movement time). Furthermore, *Sgce* sKO mice did not exhibit significant differences in vertical activity, vertical movement number or vertical time, suggesting no significant OCD-like behaviors (29). *Sgce* sKO mice showed no significant alteration either in the central time or the central distance ratio, suggesting no significant anxiety-like behaviors (29).

Significant motor deficits and lack of myoclonus in *Sgce* sKO mice

Motor coordination and balance was assessed by the beam-walking test, which is an indirect test for dystonia in mice (2,55), and accelerated rotarod tests. Mice were trained to transverse a medium square beam for 2 days. The trained mice were tested twice on four different beams and total numbers of hindpaw slips were analyzed. *Sgce* sKO mice showed 84% more slip numbers in the beam-walking test (Fig. 6A; $P = 0.047$), suggesting deficits in motor coordination and balance. We further analyzed the motor performance by accelerated rotarod test. Each mouse was put on the accelerated rotarod and the latency to fall was measured. Since mice can hold the rotarod with four paws, the latency to fall is an indicator of total motor performance and shorter latency indicates motor deficits. *Sgce* sKO mice showed a significant decrease in latency to fall at the third and fifth trials in accelerated rotarod test (Fig. 6B; $P = 0.0008$ and $P = 0.039$, respectively). Overall, *Sgce* sKO mice showed significant shorter total latency to fall (47% of WT mice) in the accelerated rotarod test (Fig. 6C; $P = 0.001$), suggesting deficits in motor learning, coordination and balance.

Since *Sgce* KO mice exhibit spontaneous myoclonus in the restrainers (29), we used the same protocol to examine the spontaneous myoclonus in *Sgce* sKO mice. *Sgce* sKO mice did not exhibit significant myoclonus compared with their control littermates (Fig. 6D; *Sgce* sKO, $P = 0.91$), suggesting that the loss of ε-sarcoglycan in the striatum alone does not produce myoclonus.

DISCUSSION

DYT11 M-D is caused by mutations in *SGCE* and exhibit myoclonus as a major symptom, and dystonia and psychiatric symptoms as secondary symptoms. *Sgce* KO mice show myoclonus, motor deficits and alterations of emotional responses and monoamine contents in the striatum, suggesting that functional alterations in the striatum may contribute to DYT11 M-D (29). However, it was not clear whether the complex symptoms are really caused by the loss of ε-sarcoglycan in the striatum itself or an end result transmitted from other brain regions. In the present study, abnormal nuclear envelopes were found in *Sgce* KO mouse striata in advance of the onset of motor deficits. To analyze the function of ε-sarcoglycan in the striatum, we produced *Sgce* sKO mice and examined their phenotypes. *Sgce* sKO mice exhibited motor deficits in both beam-walking and accelerated rotarod tests, while they did not exhibit abnormal nuclear envelopes, alteration in locomotion or myoclonus. The results suggest that ε-sarcoglycan in the striatum contribute to motor

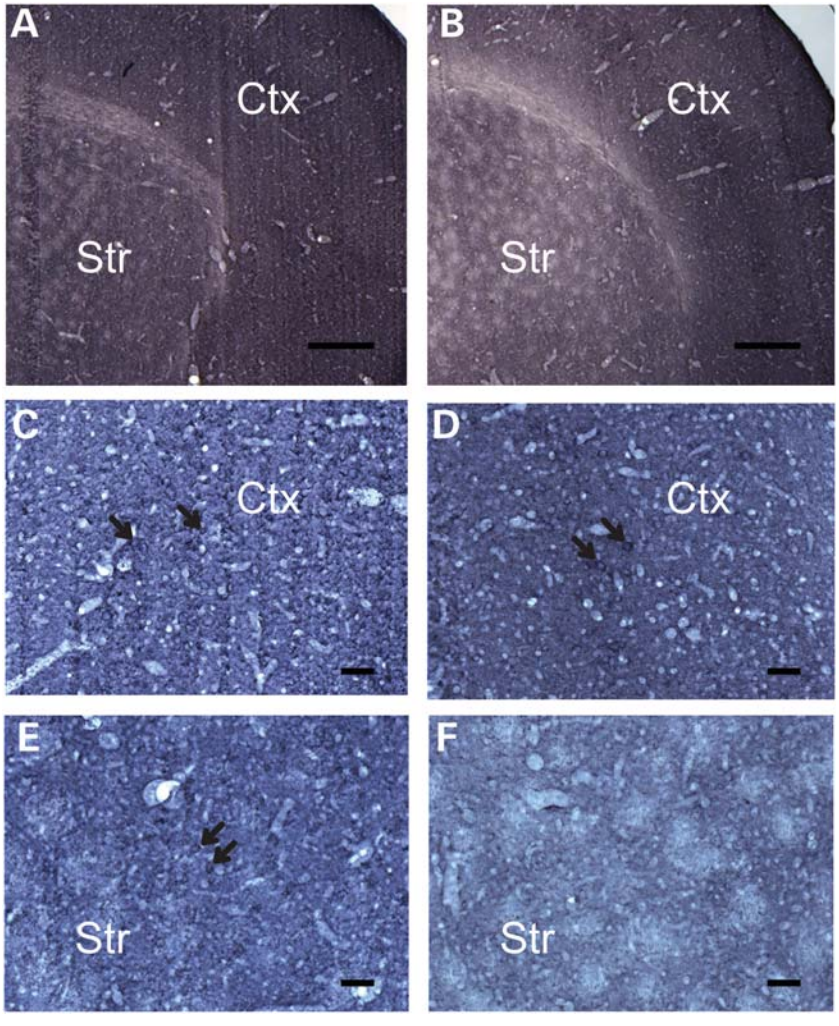

Figure 4. Immunohistochemistry using mouse monoclonal ε-sarcoglycan antibody for *Sgce* sKO mice. (**A**) A representative immunohistochemistry image of a coronal section of the brain from a control littermate of the *Sgce* sKO mouse. (**B**) A representative immunohistochemistry image of a coronal section of the brain from a *Sgce* sKO mouse. The striatum and cerebral cortex are indicated as Str and Ctx, respectively. Scale bars represent 360 μm in (A) and (B) which were captured with ×2.5 objective lens. Enlarged images captured with ×20 objective lens showed that the cortical neurons in both control (**C**) and *Sgce* sKO mice (**D**) were similarly stained as predicted. On the other hand, the striatal neurons were stained in control mice (**E**), while striatal neurons were not well stained in *Sgce* sKO mice (**F**). The results suggest striatum-specific loss of ε-sarcoglycan in *Sgce* sKO mice. Scale bars represent 48 μm in (C–F).

performance, while the loss of ε-sarcoglycan in the striatum alone does not cause the other phenotypes. The results also suggest that ε-sarcoglycan functions in multiple brain regions and contribute to their different functions. Development of therapies targeting the striatum to compensate for the loss of ε-sarcoglycan function may rescue the motor symptoms in DYT11 M-D. Future mechanistic studies focusing on the striatum will generate further insight into the pathogenesis of DYT11 M-D.

Although mutations in the genes for α-, β-, γ- and δ-sarcoglycan contribute to muscular dystrophies, *SGCE* mutations cause nervous system disorders, such as myoclonus, dystonia and psychiatric symptoms, suggesting a unique function of ε-sarcoglycan in the central nervous system and consistent with their central localization to the synapses (16). Immunoprecipitation analysis by using expression vectors in CHO cells suggested that ε-sarcoglycan is a functional homolog of α-sarcoglycan, and that it exists in two types of complexes, ε–β–γ–δ and ε–β–ζ–δ, associated with dystroglycan (23). Since the loss of one of the members in the sarcoglycan complex generally causes significant reduction in the other members in muscles (11), the loss of ε-sarcoglycan should cause reduction in the other members in the complex *in vivo*. Here, we found that the loss of ε-sarcoglycan did not affect the expression levels of α-, δ- and ζ-sarcoglycans in the mouse striatum. The results suggest that ε-sarcoglycan does not affect the stability or expression of the sarcoglycan complex. Since ε-sarcoglycan does not make a complex with α-sarcoglycan, it is expected that the loss of ε-sarcoglycan does not affect the α-sarcoglycan level in *Sgce* KO mice. On the other hand, the loss of ε-sarcoglycan did not affect δ-sarcoglycan or ζ-sarcoglycan levels in *Sgce* KO mice, either. According to the sarcoglycanopathy hypothesis (11), the loss of a member of the sarcoglycan complex should affect the stability of the complex and reduce amounts of other members. Therefore, the results suggest

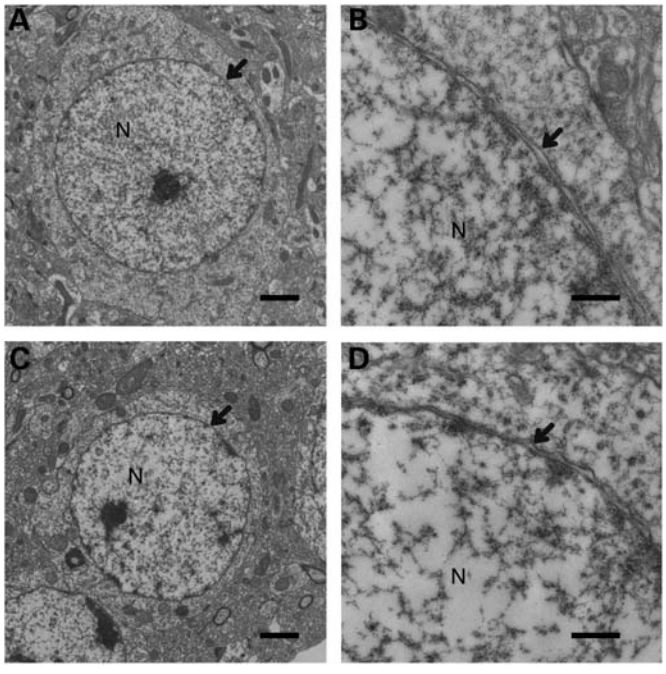

Figure 5. Nuclear envelope structures in *Sgce* sKO mice. Representative images of nuclear envelope structures in WT littermates (**A** and **B**) and *Sgce* sKO (**C** and **D**) mice are shown. Nuclear envelopes were normal in the examined nuclear envelopes. Nucleus is indicated as *N* in each panel. Arrows indicate nuclear envelopes. Magnifications: (A) and (C) are ×5K; (B) and (D) are ×25K. Scale bars indicate 2 μm in (A) and (C), and 500 nm in (B) and (D), respectively.

Table 1. Open-field behavior of CT and Sgce sKO mice

Open-field parameters	CT	*Sgce* sKO	*P*-value
Horizontal activity (beam breaks)	3394 ± 198	3581 ± 182	0.493
Total distance (cm)	1779 ± 150	1878 ± 138	0.631
Horizontal movement number	170 ± 8	174 ± 7	0.693
Horizontal movement time (s)	190 ± 14	204 ± 13	0.458
Rest time (s)	710 ± 14	696 ± 13	0.460
Clockwise revolutions (count)	6 ± 1	6 ± 1	0.731
Anticlockwise revolutions (count)	7 ± 1	7 ± 1	0.503
Vertical activity (beam breaks)	128 ± 15	146 ± 14	0.390
Vertical movement number	53 ± 5	57 ± 5	0.599
Vertical movement time (s)	57 ± 6	61 ± 5	0.607
Central time (s)	135 ± 23	146 ± 21	0.727
Central distance ratio	0.24 ± 0.02	0.24 ± 0.02	0.925
Stereotypic activity (beam breaks)	−0.05 ± 0.10	0.00 ± 0.00	0.603
Stereotypic movement number	144 ± 5	150 ± 4	0.292
Stereotypic movement time (s)	202 ± 12	208 ± 11	0.750

The values of each parameter in the open-field test are shown as means ± standard errors. Stereotypic activity was analyzed after natural log transformation to fit a normal distribution.

that ε-sarcoglycan may make a unique complex, rather than the ε–β–γ–δ or ε–β–ζ–δ complex, in the brain. The nature of the ε-sarcoglycan complex and their interacting proteins in the brain remain to be characterized.

Abnormal nuclear envelopes have been reported in DYT1 dystonia models, but not in patients. Over-expression of mutant torsinA leads to abnormal nuclear envelopes in transfected cells (32–34). Abnormal nuclear envelopes were detected in newborn *Dyt1* ΔGAG homozygous KI mice and KO mice, which exhibit neonatal lethality (36,38). Abnormal nuclear envelopes were not detected in *Dyt1* ΔGAG heterozygous KI mice, and only heterozygous mutations have been reported in human mutation carriers (36,50). Moreover, both transgenic mice over-expressing human WT torsinA and torsinA$^{\Delta E}$ exhibit abnormal nuclear envelopes (37). Therefore, the relationship between the mutation, abnormal nuclear envelopes and motor symptoms are not clear in DYT1 dystonia. Furthermore, it was not known whether the abnormal nuclear envelope exists in DYT11 M-D. Here we found that *Sgce* KO mice exhibited abnormal nuclear envelopes in MSNs in advance of onset of motor deficits. The results suggest that DYT11 M-D can be categorized into nuclear envelopathies (56). On the other hand, *Sgce* sKO mice exhibited motor deficits without abnormal nuclear envelopes. Therefore, abnormal nuclear envelopes in *Sgce* KO mice may not be caused by loss of ε-sarcoglycan function in the striatum alone; instead, it may be caused by loss of ε-sarcoglycan in other cells. Abnormal nuclear envelopes may associate with more severe alterations of neuronal circuits in *Sgce* KO mice.

DYT11 M-D patients exhibit myoclonus, dystonia and psychiatric symptoms. Consistent with the symptoms, *Sgce* KO mice exhibit myoclonus, motor deficits and alteration in emotional responses. Reduced striatal D2 binding was reported in *SGCE* mutation carriers (49), and *Sgce* KO mice also exhibit alterations in striatal monoamine metabolism (29), suggesting functional alterations in the striatum. Although ε-sarcoglycan is expressed in multiple brain regions, contribution of loss of ε-sarcoglycan to each phenotype was not known. In the present study, *Sgce* sKO mice exhibited motor deficits in both the beam-walking and accelerated rotarod tests, while they did not exhibit abnormal nuclear envelopes, alteration in locomotion or myoclonus. The results suggest that striatal ε-sarcoglycan contribute to fine motor performance, while the loss of ε-sarcoglycan in the striatum alone may not cause the other phenotypes. The results also suggest that ε-sarcoglycan functions in multiple brain regions which contribute different functions. Development of therapies targeting the striatum to compensate for the loss of ε-sarcoglycan function may rescue the motor symptoms in DYT11 M-D. Additionally, *Sgce* KO mice exhibit abnormal nuclear envelope in advance of onset of motor deficits, while *Sgce* sKO mice exhibit motor deficits without abnormal nuclear envelope. These results suggest that the striatal abnormal nuclear envelope does not associate with the motor deficits.

Myoclonus is a complex disease and caused by various etiologies. The motor cortex is the most common myoclonus source, but origins from subcortical areas, brainstem, spinal and peripheral nervous system also occur (5). Identification of affected brain circuits is important to elucidate the mechanism of myoclonus in DYT11 M-D and to develop effective treatment. Several neurophysiological studies have been reported on the affected brain regions in DYT11 M-D patients (57–60). Although neurophysiological approaches are

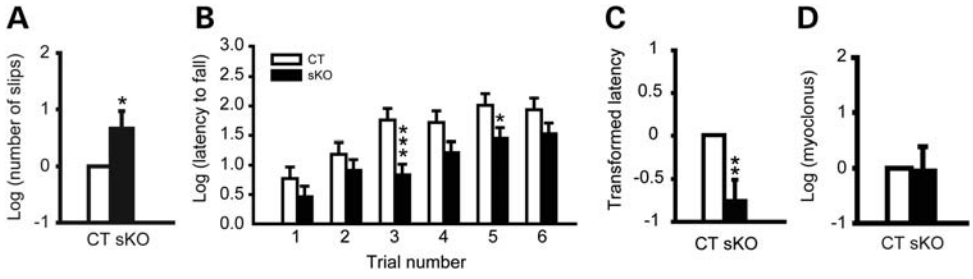

Figure 6. Behavior tests in *Sgce* sKO mice (sKO) and control littermates (CT). (**A**) Beam-walking performances in *Sgce* sKO mice and their control littermates. *Sgce* sKO mice showed significant increased slip numbers in the beam-walking test, suggesting motor deficits. (**B**) Latencies to fall in each trial of accelerated rotarod test are plotted. Trials 1–3 were performed on the first day and trials 4–6 were performed on the second day. *Sgce* sKO mice exhibited significantly shorter latency to fall in trials 3 and 5 comparing to their control littermates. (**C**) Total latency to fall in the accelerated rotarod test. The data were analyzed after natural log transformation and the data in the control littermates were normalized to zero. *Sgce* sKO mice exhibited significant decreased total latency to fall, suggesting motor deficits. (**D**) Spontaneous myoclonus in *Sgce* sKO mice. The total spontaneous myoclonus numbers in 30 min were compared with those in control littermates. The myoclonus numbers in control littermates were normalized to zero. No significant difference was detected between *Sgce* sKO mice and their control littermates. Vertical bars represent means ± SE. $^{*}P < 0.05$, $^{**}P < 0.01$. $^{***}P < 0.001$.

powerful tools to locate the brain region with altered activity, activity alteration does not necessarily mean the effect is due to loss of ε-sarcoglycan in that specific region because of the complex influence of neural circuits. Genetic dissection using tissue-specific and cell type-specific conditional KO mice is another approach to study the pathophysiology of myoclonus. In the present study, we examined myoclonus in *Sgce* sKO mice and found that *Sgce* sKO mice did not exhibit myoclonus, suggesting that the loss of ε-sarcoglycan in the striatum alone does not cause myoclonus. Since *Sgce* KO mice exhibit spontaneous myoclonus (29), the results suggest that the loss of ε-sarcoglycan in other brain regions may contribute to myoclonus. The results also suggest that the motor deficits in *Sgce* sKO mice assessed by the accelerated rotarod and beam-walking tests were not caused by myoclonus but were pure deficits of motor learning, coordination and balance that involve striatal circuits that are independent of the pathogenesis of myoclonus.

MATERIALS AND METHODS

Animals

Paternally inherited *Sgce* KO mice and WT littermates were produced and genotyped as described previously (17). *Sgce loxP neo* (17) and *Rgs9-cre* (53) mice were also prepared as described previously. *Sgce loxP neo* mice were crossed with *FLP* mice (Jackson Laboratory, Stock No. 003946) to remove *PGKneo* cassette flanked by *FRT* sites (61). *FLP* was removed by backcrossing with C57BL/6 mice to produce *Sgce loxP* mice. *Sgce loxP* male mice were crossed with *Rgs9-cre* female mice to produce *Sgce* sKO mice. The genotyping of *Sgce* sKO mice and their littermates was performed by multiplex PCR using tail DNA with a combination of SgceloxP5/SgceloxP3 (17) and creA/cre6 (62) primers. Tissue-specific deletion of *Sgce* exon 4 was confirmed by multiplex PCR using DNA isolated from the olfactory bulb, striatum, cerebral cortex, hippocampus, thalamus, medulla, cerebellar cortex and spinal cord from a *Sgce* sKO mouse. The multiplex PCR was performed by 40 cycles at 65°C of annealing temperature with SgceE4U and SgceE4D primer sets for *Sgce* exon 4-deleted locus (17) and DAT-Up (5′-TCCATAGCCAATCTCTCCAGTC-3′) and DAT-Lwt (5′-TTGATGAGGGTGGAGTTGGTCA-3′) primer sets for dopamine transporter gene as an internal control. A group of 16 *Sgce* sKO (8 males and 8 females) and 17 control littermates (7 males and 10 females) from 152 to 231 days old were used for behavioral semi-quantitative assessments of motor disorders. The open-field test was performed at 159 to 238 days old. Beam-walking test was performed at 167–246 days old. The accelerated rotarod test was performed at 173–252 days old. Finally, the myoclonus test was performed at 192–271 days old. All behavioral tests were performed by investigators blind to the genotypes. All experiments were carried out in compliance with the USPHS Guide for Care and Use of Laboratory Animals and approved by the IACUC at the University of Illinois at Urbana-Champaign (UIUC) and the University of Alabama at Birmingham (UAB).

Antibodies and western blot

Mouse α-sarcoglycan monoclonal antibody (Vector, VP-A105), rabbit δ-sarcoglycan polyclonal antibody (Santa cruz, sc-25281) and rabbit ζ-sarcoglycan antibody (Sigma-aldrich, HPA017585) were used as the primary antibodies. Bovine anti-mouse IgG-horseradish peroxidase (HRP; Santa Cruz, sc-2371) or bovine anti-rabbit IgG-HRP (Santa Cruz, sc-2370) were used as the secondary antibodies as appropriate. Striatal protein extracts were prepared from *Sgce* KO mice ($n = 6$) and their WT littermates ($n = 7$), and western blot was performed as described earlier (50). The bands were detected by SuperSignal West Pico Chemiluminescent Substrate (Thermo Scientific). Levels of glyceraldehyde-3-phosphate dehydrogenase (GAPDH) were also detected with HRP-conjugated GAPDH antibody (Santa Cruz, sc-25778 HRP) as a loading control. Restore Western Blot Stripping buffer (Thermo Scientific) was used for stripping GAPDH antibody to detect sarcoglycans. Western blot was performed in more than duplicate. The signals were captured by Alpha Innotech FluorChem FC2 and quantified with UN-SCAN-IT gel software (Silk Scientific).

Immunohistochemistry

We recently developed a high-specific mouse monoclonal antibody against mouse ε-sarcoglycan (mSE 3A9). This

antibody detected only single strong band at 52 kDa in the striatal protein extract from WT mice, while it did not detect any band in the striatal protein extract from *Sgce* KO mice in western blot analysis (50). We used this antibody for immunohistochemistry. Brains were obtained from *Sgce* sKO and control littermate mice and processed as described earlier (31). The brains were frozen using dry-ice powder and cut into 40 μm sections with a Histoslide 2000 sliding microtome (Reichert-Jung). Sections were stained with the mouse monoclonal ε-sarcoglycan antibody (mSE 3A9; 1 μg/ml), Vectastain ABC kit for peroxidase mouse IgG and DAB peroxidase substrate kit with nickel solution (Vector Lab). Images were captured using ZEISS Axiophot RZGF-1 microscope with ×2.5 or ×20 Plan-NEOFLUAR objective lens and MBF Bioscience Neurolucida 7 software (MicroBrightField, Inc).

Transmission electron microscopy analysis

Brain sections for transmission electron microscope were prepared as described earlier (50). *Sgce* KO mice and their WT littermates ($n = 6$ each, ∼2 to 5.5 months of age) were perfused with chilled 0.1 M phosphate-buffered saline (pH 7.4) followed by Karnovsky's Fixative in phosphate-buffered 2% glutaraldeyde and 2.5% paraformaldehyde. The brains were dissected out and left in Karnovsky's Fixative overnight. The tissue was then trimmed and washed in cacodylate buffer with no further additives. Microwave fixation was used with the secondary 2% osmium tetroxide fixative, followed by the addition of 3% potassium ferricyanide for 30 min. After washing with water, saturated uranyl acetate was added for en bloc staining. The tissue was dehydrated in a series of increasing concentrations of ethanol starting at 50%. Acetonitrile was used as the transition fluid between ethanol and the epoxy. Infiltration series was done with an epoxy mixture using the epon substitute Lx112. The resulting blocks were polymerized at 90°C overnight, trimmed with a razor blade and ultrathin sectioned with diamond knives. Sections were then stained with uranyl acetate and lead citrate, and examined or photographed with a Hitachi H600 transmission electron microscope. *Sgce* sKO mice and CT adult mice ($n = 3$ each) were also perfused and processed. Sections were examined or photographed with a Hitachi 7600 transmission electron microscope with digital camera. The nuclear envelopes in MSNs were examined by investigators blind to the genotypes.

Behavioral semi-quantitative assessments of motor disorders

Behavioral semi-quantitative assessments of motor disorders were performed as previously described (46,54). The mouse was placed on the table and assessments of hindpaw clasping, hindpaw dystonia, truncal dystonia and balance adjustments to a postural challenge were made. The hindpaw clasping was assessed as hindlpaw movements for postural adjustment and attempt to straighten up while the mouse was suspended by the mid-tail.

Open-field test

Open-field test was performed during the light period as previously described (29,63). In brief, spontaneous activities of individual mice were recorded by infrared light beam sensors in a 41 × 41 × 31 cm acryl case for 15 min at 1 min intervals using DigiPro software (AccuScan Instruments).

Beam-walking test

Beam-walking test was performed as described earlier (29,46,47,50,55,64). In brief, mice were trained to transverse a medium square beam (14 mm wide) in three consecutive trials each day for 2 days. The trained mice were tested twice on the medium square beam and medium round beam (17 mm diameter) on the third day, and small round beam (10 mm diameter) and small square beam (7 mm wide) on the fourth day. The hindpaw slips on each side were recorded.

Accelerated rotarod test

The motor performance was examined with Economex accelerating rotarod (Columbus Instruments) as previously described (46) with minor modification. The apparatus started at an initial speed of 4 rpm, and then each mouse was put on the same slot one by one, instead of putting four mice on the different slots on the apparatus. The rod speed was gradually accelerated at a rate of 0.2 rpm/s. The latency to fall was measured with a cutoff time of 2 min. Mice were tested for three trials on each day for 2 days. The trials within the same day were performed at ∼1 h intervals.

Spontaneous myoclonus test

Mice were placed in transparent flat bottom rodent restrainers (model 541-RR; Plas-labs, Inc., MI, USA) to minimize voluntary movements and videotaped for an hour. The mice were habituated for ∼30 min in the restrainers and the numbers of spontaneous myoclonus jerks of the whole body were counted during the subsequent 30 min as previously described (29).

Statistics

Numbers of MSN sections with abnormal nuclear envelopes and those with normal nuclear envelopes were analyzed between *Sgce* KO and WT mice using the Chi-square test. Data from the open-field test were analyzed by the analysis of variance mixed model with SAS program as previously described (46). Stereotypic activity was analyzed after natural log transformation to obtain a normal distribution. Total latency to fall in the accelerated rotarod test, the numbers of myoclonus and the beam-walking data were analyzed after natural log transformation to obtain normal distribution using logistic regression (GENMOD) with negative binominal distribution using GEE model in the software for repeated measurements (29,46,64). Sex, age and body weight were input as variables. The data in the control littermates were normalized to zero, except in case of latency to fall in each trial of accelerated rotarod test, which was

estimated by the mixed model after natural log transformation of the latency. The density of α-sarcoglycan, δ-sarcoglycan or ζ-sarcoglycan bands was standardized to that of GAPDH. The standardized pixel ratios were analyzed by Student's *t*-test. The data in the control WT littermates were normalized to 100%. Significance was assigned at $P < 0.05$.

ACKNOWLEDGEMENTS

We thank Lisa Foster, Andrea McCullough and their staff for animal care, Lou Ann Miller, Dr Guang Yang, JinDong Li, Dr Huan-Xin Chen, Miki Jinno, Jennifer Neighbors, Veena Ganesh and Mark P. DeAndrade for their technical assistance. We also thank Dr William T. Dauer for his technical advice on identifying the abnormal nuclear envelopes.

Conflict of Interest statement. None declared.

FUNDING

This work was supported by National Institutes of Health (NS47692, NS54246, NS57098, NS47466, NS37406, NS65273, NS72876 and NS74423); and the startup funds from the Lucille P. Markey Charitable Trust (UIUC), Department of Neurology (UAB) and Tyler's Hope for a Dystonia Cure, Inc. (UF).

REFERENCES

1. Fahn, S. (1988) Concept and classification of dystonia. *Adv. Neurol.*, **50**, 1–8.
2. Breakefield, X.O., Blood, A.J., Li, Y., Hallett, M., Hanson, P.I. and Standaert, D.G. (2008) The pathophysiological basis of dystonias. *Nat. Rev. Neurosci.*, **9**, 222–234.
3. Camargos, S., Scholz, S., Simon-Sanchez, J., Paisan-Ruiz, C., Lewis, P., Hernandez, D., Ding, J., Gibbs, J.R., Cookson, M.R., Bras, J. *et al.* (2008) DYT16, a novel young-onset dystonia-parkinsonism disorder: identification of a segregating mutation in the stress-response protein PRKRA. *Lancet Neurol.*, **7**, 207–215.
4. Fuchs, T., Gavarini, S., Saunders-Pullman, R., Raymond, D., Ehrlich, M.E., Bressman, S.B. and Ozelius, L.J. (2009) Mutations in the THAP1 gene are responsible for DYT6 primary torsion dystonia. *Nat. Genet.*, **41**, 286–288.
5. Caviness, J.N. and Brown, P. (2004) Myoclonus: current concepts and recent advances. *Lancet Neurol.*, **3**, 598–607.
6. Kinugawa, K., Vidailhet, M., Clot, F., Apartis, E., Grabli, D. and Roze, E. (2009) Myoclonus-dystonia: an update. *Mov. Disord.*, **24**, 479–489.
7. Valente, E.M., Misbahuddin, A., Brancati, F., Placzek, M.R., Garavaglia, B., Salvi, S., Nemeth, A., Shaw-Smith, C., Nardocci, N., Bentivoglio, A.R. *et al.* (2003) Analysis of the epsilon-sarcoglycan gene in familial and sporadic myoclonus-dystonia: evidence for genetic heterogeneity. *Mov. Disord.*, **18**, 1047–1051.
8. Han, F., Racacho, L., Lang, A.E., Bulman, D.E. and Grimes, D.A. (2007) Refinement of the DYT15 locus in myoclonus dystonia. *Mov. Disord.*, **22**, 888–892.
9. Zimprich, A., Grabowski, M., Asmus, F., Naumann, M., Berg, D., Bertram, M., Scheidtmann, K., Kern, P., Winkelmann, J., Muller-Myhsok, B. *et al.* (2001) Mutations in the gene encoding epsilon-sarcoglycan cause myoclonus-dystonia syndrome. *Nat. Genet.*, **29**, 66–69.
10. Sandona, D. and Betto, R. (2009) Sarcoglycanopathies: molecular pathogenesis and therapeutic prospects. *Expert Rev. Mol. Med.*, **11**, e28.
11. Ozawa, E., Noguchi, S., Mizuno, Y., Hagiwara, Y. and Yoshida, M. (1998) From dystrophinopathy to sarcoglycanopathy: evolution of a concept of muscular dystrophy. *Muscle Nerve*, **21**, 421–438.
12. Laval, S.H. and Bushby, K.M. (2004) Limb-girdle muscular dystrophies—from genetics to molecular pathology. *Neuropathol. Appl. Neurobiol.*, **30**, 91–105.
13. Wheeler, M.T., Zarnegar, S. and McNally, E.M. (2002) Zeta-sarcoglycan, a novel component of the sarcoglycan complex, is reduced in muscular dystrophy. *Hum. Mol. Genet.*, **11**, 2147–2154.
14. Ettinger, A.J., Feng, G. and Sanes, J.R. (1997) epsilon-Sarcoglycan, a broadly expressed homologue of the gene mutated in limb-girdle muscular dystrophy 2D. *J. Biol. Chem.*, **272**, 32534–32538.
15. Ettinger, A.J., Feng, G. and Sanes, J.R. (1998) Additions and Corrections to epsilon-Sarcoglycan, a broadly expressed homologue of the gene mutated in limb-girdle muscular dystrophy 2D. *J. Biol. Chem.*, **273**, 19922.
16. Nishiyama, A., Endo, T., Takeda, S. and Imamura, M. (2004) Identification and characterization of epsilon-sarcoglycans in the central nervous system. *Brain Res. Mol. Brain Res.*, **125**, 1–12.
17. Yokoi, F., Dang, M.T., Mitsui, S. and Li, Y. (2005) Exclusive paternal expression and novel alternatively spliced variants of epsilon-sarcoglycan mRNA in mouse brain. *FEBS Lett.*, **579**, 4822–4828.
18. McNally, E.M., Ly, C.T. and Kunkel, L.M. (1998) Human epsilon-sarcoglycan is highly related to alpha-sarcoglycan (adhalin), the limb girdle muscular dystrophy 2D gene. *FEBS Lett.*, **422**, 27–32.
19. Ritz, K., van Schaik, B.D., Jakobs, M.E., van Kampen, A.H., Aronica, E., Tijssen, M.A. and Baas, F. (2011) SGCE isoform characterization and expression in human brain: implications for myoclonus-dystonia pathogenesis? *Eur. J. Hum. Genet.*, **19**, 438–444.
20. Xiao, J. and LeDoux, M.S. (2003) Cloning, developmental regulation and neural localization of rat epsilon-sarcoglycan. *Brain Res. Mol. Brain Res.*, **119**, 132–143.
21. Dickens, N.J., Beatson, S. and Ponting, C.P. (2002) Cadherin-like domains in alpha-dystroglycan, alpha/epsilon-sarcoglycan and yeast and bacterial proteins. *Curr. Biol.*, **12**, R197–R199.
22. Sheng, M. and Sala, C. (2001) PDZ domains and the organization of supramolecular complexes. *Annu. Rev. Neurosci.*, **24**, 1–29.
23. Shiga, K., Yoshioka, H., Matsumiya, T., Kimura, I., Takeda, S. and Imamura, M. (2006) Zeta-sarcoglycan is a functional homologue of gamma-sarcoglycan in the formation of the sarcoglycan complex. *Exp. Cell Res.*, **312**, 2083–2092.
24. Grabowski, M., Zimprich, A., Lorenz-Depiereux, B., Kalscheuer, V., Asmus, F., Gasser, T., Meitinger, T. and Strom, T.M. (2003) The epsilon-sarcoglycan gene (SGCE), mutated in myoclonus-dystonia syndrome, is maternally imprinted. *Eur. J. Hum. Genet.*, **11**, 138–144.
25. Piras, G., El Kharroubi, A., Kozlov, S., Escalante-Alcalde, D., Hernandez, L., Copeland, N.G., Gilbert, D.J., Jenkins, N.A. and Stewart, C.L. (2000) Zac1 (Lot1), a potential tumor suppressor gene, and the gene for epsilon-sarcoglycan are maternally imprinted genes: identification by a subtractive screen of novel uniparental fibroblast lines. *Mol. Cell Biol.*, **20**, 3308–3315.
26. Muller, B., Hedrich, K., Kock, N., Dragasevic, N., Svetel, M., Garrels, J., Landt, O., Nitschke, M., Pramstaller, P.P., Reik, W. *et al.* (2002) Evidence that paternal expression of the epsilon-sarcoglycan gene accounts for reduced penetrance in myoclonus-dystonia. *Am. J. Hum. Genet.*, **71**, 1303–1311.
27. Lancioni, A., Luisa Rotundo, I., Monique Kobayashi, Y., D'Orsi, L., Aurino, S., Nigro, G., Piluso, G., Acampora, D., Cacciottolo, M., Campbell, K.P. *et al.* (2011) Combined deficiency of alpha and epsilon sarcoglycan disrupts the cardiac dystrophin complex. *Hum. Mol. Genet.*, **20**, 4644–4654.
28. Hedrich, K., Meyer, E.M., Schule, B., Kock, N., de Carvalho Aguiar, P., Wiegers, K., Koelman, J.H., Garrels, J., Durr, R., Liu, L. *et al.* (2004) Myoclonus-dystonia: detection of novel, recurrent, and de novo SGCE mutations. *Neurology*, **62**, 1229–1231.
29. Yokoi, F., Dang, M.T., Li, J. and Li, Y. (2006) Myoclonus, motor deficits, alterations in emotional responses and monoamine metabolism in epsilon-sarcoglycan deficient mice. *J. Biochem.*, **140**, 141–146.
30. Carbon, M., Kingsley, P.B., Su, S., Smith, G.S., Spetsieris, P., Bressman, S. and Eidelberg, D. (2004) Microstructural white matter changes in carriers of the DYT1 gene mutation. *Ann. Neurol.*, **56**, 283–286.
31. Yokoi, F., Dang, M.T., Miller, C.A., Marshall, A.G., Campbell, S.L., Sweatt, J.D. and Li, Y. (2009) Increased c-fos expression in the central nucleus of the amygdala and enhancement of cued fear memory in Dyt1 DeltaGAG knock-in mice. *Neurosci. Res.*, **65**, 228–235.

32. Naismith, T.V., Heuser, J.E., Breakefield, X.O. and Hanson, P.I. (2004) TorsinA in the nuclear envelope. *Proc. Natl Acad. Sci. USA*, **101**, 7612–7617.
33. Gonzalez-Alegre, P. and Paulson, H.L. (2004) Aberrant cellular behavior of mutant torsinA implicates nuclear envelope dysfunction in DYT1 dystonia. *J. Neurosci.*, **24**, 2593–2601.
34. Goodchild, R.E. and Dauer, W.T. (2004) Mislocalization to the nuclear envelope: an effect of the dystonia-causing torsinA mutation. *Proc. Natl Acad. Sci. USA*, **101**, 847–852.
35. Nery, F.C., Zeng, J., Niland, B.P., Hewett, J., Farley, J., Irimia, D., Li, Y., Wiche, G., Sonnenberg, A. and Breakefield, X.O. (2008) TorsinA binds the KASH domain of nesprins and participates in linkage between nuclear envelope and cytoskeleton. *J. Cell Sci.*, **121**, 3476–3486.
36. Goodchild, R.E., Kim, C.E. and Dauer, W.T. (2005) Loss of the dystonia-associated protein torsinA selectively disrupts the neuronal nuclear envelope. *Neuron*, **48**, 923–932.
37. Grundmann, K., Reischmann, B., Vanhoutte, G., Hubener, J., Teismann, P., Hauser, T.K., Bonin, M., Wilbertz, J., Horn, S., Nguyen, H.P. *et al.* (2007) Overexpression of human wildtype torsinA and human DeltaGAG torsinA in a transgenic mouse model causes phenotypic abnormalities. *Neurobiol. Dis.*, **27**, 190–206.
38. Yokoi, F., Dang, M.T., Li, J., Standaert, D.G. and Li, Y. (2011) Motor deficits and decreased striatal dopamine receptor 2 binding activity in the striatum-specific *Dyt1* conditional knockout mice. *PLoS ONE*, **6**, e24539.
39. Kim, C.E., Perez, A., Perkins, G., Ellisman, M.H. and Dauer, W.T. (2010) A molecular mechanism underlying the neural-specific defect in torsinA mutant mice. *Proc. Natl Acad. Sci. USA*, **107**, 9861–9866.
40. Tolosa, E. and Compta, Y. (2006) Dystonia in Parkinson's disease. *J. Neurol.*, **253**(Suppl. 7), VII7–VII13.
41. Abdo, W.F., van de Warrenburg, B.P., Burn, D.J., Quinn, N.P. and Bloem, B.R. (2010) The clinical approach to movement disorders. *Nat. Rev. Neurol.*, **6**, 29–37.
42. Braak, H., Ghebremedhin, E., Rub, U., Bratzke, H. and Del Tredici, K. (2004) Stages in the development of Parkinson's disease-related pathology. *Cell Tissue Res.*, **318**, 121–134.
43. Shoulson, I. and Young, A.B. (2011) Milestones in huntington disease. *Mov. Disord.*, **26**, 1127–1133.
44. Segawa, M. (2009) Autosomal dominant GTP cyclohydrolase I (AD GCH 1) deficiency (Segawa disease, dystonia 5; DYT 5). *Chang Gung Med. J.*, **32**, 1–11.
45. Augood, S.J., Hollingsworth, Z., Albers, D.S., Yang, L., Leung, J.C., Muller, B., Klein, C., Breakefield, X.O. and Standaert, D.G. (2002) Dopamine transmission in DYT1 dystonia: a biochemical and autoradiographical study. *Neurology*, **59**, 445–448.
46. Dang, M.T., Yokoi, F., McNaught, K.S., Jengelley, T.A., Jackson, T., Li, J. and Li, Y. (2005) Generation and Characterization of Dyt1 deltaGAG Knock-in Mouse as a Model for Early-Onset Dystonia. *Exp. Neurol.*, **196**, 452–463.
47. Dang, M.T., Yokoi, F., Pence, M.A. and Li, Y. (2006) Motor deficits and hyperactivity in Dyt1 knockdown mice. *Neurosci. Res.*, **56**, 470–474.
48. Napolitano, F., Pasqualetti, M., Usiello, A., Santini, E., Pacini, G., Sciamanna, G., Errico, F., Tassone, A., Di Dato, V., Martella, G. *et al.* (2010) Dopamine D2 receptor dysfunction is rescued by adenosine A2A receptor antagonism in a model of DYT1 dystonia. *Neurobiol. Dis.*, **38**, 434–445.
49. Beukers, R.J., Booij, J., Weisscher, N., Zijlstra, F., van Amelsvoort, T.A. and Tijssen, M.A. (2009) Reduced striatal D2 receptor binding in myoclonus-dystonia. *Eur. J. Nucl. Med. Mol. Imaging*, **36**, 269–274.
50. Yokoi, F., Yang, G., Li, J., Deandrade, M.P., Zhou, T. and Li, Y. (2010) Earlier onset of motor deficits in mice with double mutations in Dyt1 and Sgce. *J. Biochem.*, **148**, 459–466.
51. Sauer, B. and Henderson, N. (1988) Site-specific DNA recombination in mammalian cells by the Cre recombinase of bacteriophage P1. *Proc. Natl Acad. Sci. USA*, **85**, 5166–5170.
52. Schwenk, F., Baron, U. and Rajewsky, K. (1995) A cre-transgenic mouse strain for the ubiquitous deletion of loxP-flanked gene segments including deletion in germ cells. *Nucleic Acids Res.*, **23**, 5080–5081.
53. Dang, M.T., Yokoi, F., Yin, H.H., Lovinger, D.M., Wang, Y. and Li, Y. (2006) Disrupted motor learning and long-term synaptic plasticity in mice lacking NMDAR1 in the striatum. *Proc. Natl Acad. Sci. USA*, **103**, 15254–15259.
54. Fernagut, P., Diguet, E., Stefanova, N., Biran, M., Wenning, G., Canioni, P., Bioulac, B. and Tison, F. (2002) Subacute systemic 3-nitropropionic acid intoxication induces a distinct motor disorder in adult C57Bl/6 mice: behavioural and histopathological characterisation. *Neuroscience*, **114**, 1005.
55. DeAndrade, M.P., Yokoi, F., van Groen, T., Lingrel, J.B. and Li, Y. (2011) Characterization of Atp1a3 mutant mice as a model of rapid-onset dystonia with parkinsonism. *Behav. Brain Res.*, **216**, 659–665.
56. Nagano, A. and Arahata, K. (2000) Nuclear envelope proteins and associated diseases. *Curr. Opin. Neurol.*, **13**, 533–539.
57. Meunier, S., Lourenco, G., Roze, E., Apartis, E., Trocello, J.M. and Vidailhet, M. (2008) Cortical excitability in DYT-11 positive myoclonus dystonia. *Mov. Disord.*, **23**, 761–764.
58. Li, J.Y., Cunic, D.I., Paradiso, G., Gunraj, C., Pal, P.K., Lang, A.E. and Chen, R. (2008) Electrophysiological features of myoclonus-dystonia. *Mov. Disord.*, **23**, 2055–2061.
59. Roze, E., Apartis, E., Clot, F., Dorison, N., Thobois, S., Guyant-Marechal, L., Tranchant, C., Damier, P., Doummar, D., Bahi-Buisson, N. *et al.* (2008) Myoclonus-dystonia: clinical and electrophysiologic pattern related to SGCE mutations. *Neurology*, **70**, 1010–1016.
60. van der Salm, S.M., van Rootselaar, A.F., Foncke, E.M., Koelman, J.H., Bour, L.J., Bhatia, K.P., Rothwell, J.C. and Tijssen, M.A. (2009) Normal cortical excitability in Myoclonus-Dystonia—a TMS study. *Exp. Neurol.*, **216**, 300–305.
61. Farley, F.W., Soriano, P., Steffen, L.S. and Dymecki, S.M. (2000) Widespread recombinase expression using FLPeR (flipper) mice. *Genesis*, **28**, 106–110.
62. Campos, V.E., Du, M. and Li, Y. (2004) Increased seizure susceptibility and cortical malformation in beta-catenin mutant mice. *Biochem. Biophys. Res. Commun.*, **320**, 606–614.
63. Cao, B.J. and Li, Y. (2002) Reduced anxiety- and depression-like behaviors in Emx1 homozygous mutant mice. *Brain Res.*, **937**, 32–40.
64. Yokoi, F., Dang, M.T., Mitsui, S., Li, J. and Li, Y. (2008) Motor deficits and hyperactivity in cerebral cortex-specific Dyt1 conditional knockout mice. *J. Biochem.*, **143**, 39–47.